Nuclear Engineering and Technology 49 (2017) 1654–1659

Contents lists available at ScienceDirect

Nuclear Engineering and Technology

journal homepage: www.elsevier.com/locate/net

Original Article

Boundary layer analysis of persistent moving horizontal needle in Blasius and Sakiadis magnetohydrodynamic radiative nanofluid flows

Penem Mohan Krishna [a], Ram Prakash Sharma [b], Naramgari Sandeep [c, *]

[a] Department of Humanities and Sciences, Sri Venkateswara College of Engineering and Technology, Chittoor 517 127, India
[b] Department of Mathematics, JECRC University, Jaipur 303905, Rajasthan, India
[c] Department of Mathematics, VIT University, Vellore 632014, India

A R T I C L E I N F O

Article history:
Received 25 June 2017
Received in revised form
20 July 2017
Accepted 28 July 2017
Available online 24 August 2017

Keywords:
Dissipation
Heat Transfer
Joule Heating
Magnetohydrodynamics
Nanofluid
Radiation

A B S T R A C T

The boundary layer of a two-dimensional forced convective flow along a persistent moving horizontal needle in an electrically conducting magnetohydrodynamic dissipative nanofluid was numerically investigated. The energy equation was constructed with Joule heating, viscous dissipation, uneven heat source/sink, and thermal radiation effects. We analyzed the boundary layer behavior of a continuously moving needle in Blasius (moving fluid) and Sakiadis (quiescent fluid) flows. We considered Cu nanoparticles embedded in methanol. The reduced system of governing Partial differential equations (PDEs) was solved by employing the Runge–Kutta-based shooting process. Computational outcomes of the rate of heat transfer and friction factors were tabulated and discussed. Velocity and temperature descriptions were examined with the assistance of graphical illustrations. Increasing the needle size did not have a significant influence on the Blasius flow. The heat transfer rate in the Sakiadis flow was high compared with that in the Blasius flow.

1. Introduction

Nanofluids have advantages in a broad range of technical applications, and their characteristics are of interest in both science and engineering. Nanofluid technologies have potential benefits in solar energy, heat transfer fluids (cooling or heating), nuclear reactors, etc. Accordingly, in recent decades, a significant number of investigators have been engaged in studying nanofluid applications in various fields. Choi [1], for example, developed the concept of nanofluids in cooling technologies.

Among such studies, many researchers have been energetically involved in solving the problem of boundary layer flows past thin needles, including Agarwal et al. [2], Kumari and Nath [3], Ishak et al. [4], Ahmad et al. [5], Takhar et al. [6], Cebeci and Na [7], and Patil et al. [8]. Mehmood et al. [9] analyzed the oblique flow of a Jeffery nanofluid along a stretching plate. The influence of the porosity of the uniform stream and the quiescent ambient fluid motion of a nanofluid under a convective boundary condition were studied by Hady et al. [10]. Makinde [11] conducted an analysis of the quiescent ambient fluid flow of nanofluids in the presence of Newtonian heating and viscous dissipation.

Makinde and Aziz [12] investigated the numerical solution of the induced laminar flow of nanofluids past a linearly stretching sheet. Sandeep et al. [13] investigated the free convective motion of nanofluids past an impulsively vertical surface. Mohan Krishna et al. [14] studied the same topic, and extended the study by adding a heat source and various nanofluids. Sandeep [15] discussed the convective heat transfer in a magnetohydrodynamic (MHD) liquid film flow. The impact of internal friction and radiation on Sakiadis and Blasius motions under the surface boundary condition was analyzed by Olanrewaju et al. [16]. Awais et al. [17] studied the MHDs of a coupled stress nanofluid over a stretching sheet in the presence of a convective wall. Ambethkar [18] discussed the impact of an unsteady MHD natural convective motion over a vertical surface under the influence of constant suction. Nadeem et al. [19] discussed the stagnation point flow of a nanofluid using phase flow and Buongiorno models.

Mohan Krishna et al. [20] investigated the MHD boundary layer motion of a vertical surface in the presence of a heat source. Ibrahim and Makinde [21] investigated the impact of a chemical reaction on the laminar natural convective motion of a rotating vertical sheet with suction. Sulochana et al. [22] and Jones et al. [23] investigated the effect of an aligned magnetic field on laminar flow through various channels. Khan and Pop [24] conducted a

* Corresponding author.
E-mail address: dr.nsrh@gmail.com (N. Sandeep).

http://dx.doi.org/10.1016/j.net.2017.07.023

numerical study of the boundary layer motion of a nanofluid past a stretching flat surface. Bhattacharya et al. [25] explored the numerical solution of an unsteady MHD laminar flow past a stretching sheet under the assumption of suction/blowing, with chemical reaction and power-law variation in the wall concentration. Ramesh et al. [26] examined the boundary layer motion on the transfer of heat in a dusty fluid past a permeable stretching surface under the influence of a thermal radiative effect [26]. The transfer of heat and unsteady laminar motion of a stretching surface have been discussed by Sharidan et al. [27]. Siddiqa et al. [28] performed studies on the heat and mass transfer of a nanofluid with a bio-convective flow along a vertical cone. Very recently, researchers [29–31] studied the heat and mass transfer nature of MHD flows over various geometries. The heat and mass transfer characteristics of a MHD non-Newtonian nanofluid flow over different geometries were studied by various researchers [9,17,19,28].

In this study, a two-dimensional forced convective flow along a persistent moving horizontal needle in an electrically conducting MHD dissipative nanofluid was numerically investigated. The energy equation was constructed with Joule heating, viscous dissipation, and nonuniform heat source/sink effects. We have analyzed the boundary layer behavior of a continuously moving needle in the Blasius (moving fluid) and Sakiadis (quiescent fluid) flows. We considered Cu nanoparticles embedded in methanol. The reduced system of governing Partial differential equations (PDEs) was solved by employing the Runge–Kutta-based shooting process.

2. Mathematical formulation

Consider the steady, forced convective MHD Newtonian nanofluid motion under the stagnation region of a thin needle. Fig. 1 shows the cylindrical coordinates (x, r) such that the x-axis is the axial direction, and r is normal to the x-axis and termed the radial direction, while c is the magnitude of the needle. We examined the flow with the assistance of thermal stratification. We assumed that the temperature of the cylindrical surface T_w was much greater than that of the ambient fluid, and T_w and T_∞ are constants where $T_w > T_\infty$ (heated needle). In addition, $U_0 = u_w + u_\infty$ is the composite velocity along the x-axis, and the needle moves with the constant velocity u_w. The mainstream of constant velocity is u_∞. The electromagnetic field B_0 is imposed parallel to the direction of motion, and the induced magnetic field is neglected. Joule heating and the uneven heat source/sink are taken into account.

Under the above conditions and in the absence of a pressure gradient, we imposed the following governing equations:

$$(ru)_x + (rv)_r = 0 \tag{1}$$

$$\rho_{nf}(uu_x + vu_r) = \mu_{nf}\frac{1}{r}(ru_r)_r - \sigma B_0^2 u \tag{2}$$

$$(\rho C_p)_{nf}(uT_x + vT_r) = \frac{1}{r}\left[\left(k_{nf}\right)(rT_r)\right]_r + q''' + \sigma B_0^2 u^2 + \mu_f (u_r)^2 - \frac{16\sigma^* T_\infty^3}{3k^*}T_{rr} \tag{3}$$

The suitable boundary conditions are as follows:

$$\begin{aligned} &u = u_w, T = T_w\ v = 0,\ \text{at}\ r = R(x) \\ &T \to T_\infty\ , u \to u_\infty,\quad \text{as}\ r \to \infty \end{aligned} \tag{4}$$

where u and v are velocities in the axial and radial (x, r) directions, respectively; $(\rho C_p)_{nf}, k_{nf}, \rho_{nf}, \mu_{nf}$ are the specific heat capacity, thermal conductivity, effective density, and viscosity of the nanofluids, respectively, which are given as follows (see [15]):

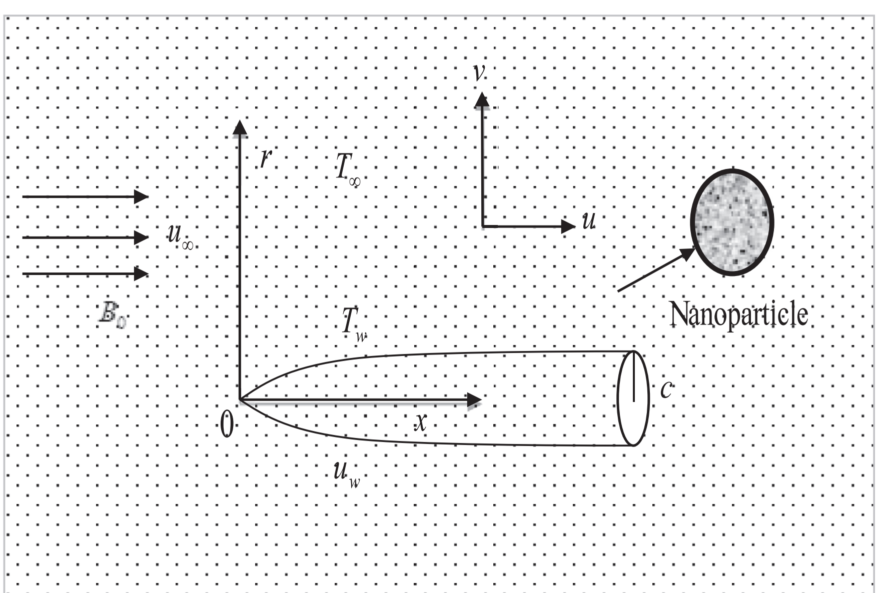

Fig. 1. Schematic representation.

$$\left.\begin{aligned} k_{nf} &= \left(\frac{k_s + 2k_f - 2\phi k_f + 2\phi k_s}{k_s + 2k_f + 2\phi k_f - 2\phi k_s}\right)k_f \\ \rho_{nf} &= \rho_f - \phi\rho_f + \phi\rho_s, \mu_{nf} = \mu_f(1-\phi)^{-2.5} \\ (\rho C_p)_{nf} &= (\rho C_p)_f - \phi(\rho C_p)_f + \phi(\rho C_p)_s \end{aligned}\right\} \tag{5}$$

The nonuniform heat source/sink is stated as $q''' = (k_f U_0(T_w - T_\infty)/x\nu_f)\left[A^* f' + B^* \frac{(T-T_\infty)}{(T_w - T_\infty)}\right]$. To compute the basic equations [Eqs. (1–3)] under the boundary restrictions [Eq. (4)], we assumed the relevant transformations as follows:

$$\psi = \nu_f x f(\eta), \eta = U_0 r^2 \big/ \nu_f x, \theta(\eta) = (T - T_\infty)/(T_w - T_\infty) \tag{6}$$

here, ψ is defined as a stream function that satisfies the continuity equation [Eq. (1)] exactly, and the velocity components are defined as $u = r^{-1}\psi_r, v = -r^{-1}\psi_x$. Assume that $\eta = c$ in Eq. (6) predicts the magnitude of the needle $r = R(x) = \sqrt{\nu_f c x / U_0}$ along the surface. Using Eq. (6) in basic Eqs. (2–4) reduces it to the following nonlinear differential form:

$$2(1-\phi)^{-2.5}(f'''\eta + f'') + \left(1 - \phi + \phi\frac{\rho_s}{\rho_f}\right)(ff'' - Mf') = 0 \tag{7}$$

$$2\left(\frac{k_{nf}}{k_f} + R\right)(\theta''\eta + \theta') + \left(1 - \phi + \phi\frac{(\rho C_p)_s}{(\rho C_p)_f}\right)\Pr f\theta' + (A^* f' + B^*\theta) + Ec\left(2\eta f''^2 + Mf'^2\right) = 0 \tag{8}$$

The suitable boundary conditions are as follows:

$$\begin{aligned} &f(c) = c\lambda/2, f'(c) = \lambda/2, \theta(c) = 1 \\ &f'(\eta) \to 1 - \lambda/2, \theta(\eta) \to (\lambda/2) \text{ as } \eta \to \infty \end{aligned} \tag{9}$$

where $\lambda = u_w/U_0$ is defined as the ratio of the velocity of the needle and the composite velocity. Here, $\lambda = 0$ and $\lambda = 1$ relate to a fixed needle in a moving fluid (Blasius flow) and a moving needle in a stationary fluid (Sakiadis flow), respectively. In this study, $\lambda \le 1$ is restricted to all boundary conditions, i.e., a free stream always moves in a positive direction. The physical parameters $M, \Pr, A^*, B^*, Ec$, and R denote the magnetic field, Prandtl number, nonuniform heat source/sink, dissipation, and thermal radiation, respectively. They are described as follows:

$$M = \frac{\sigma B_0^2}{2\rho U_0}, \Pr = \frac{\mu C_p}{k_f}, Ec = \frac{2U_0^2}{C_p(T_w - T_\infty)}, R = \frac{16\sigma^* T_\infty^3}{3k^* k} \tag{10}$$

The friction factor is given by the following equation:

$$\mathrm{Re}_x^{1/2} C_f = 4c^{1/2}(1-\phi)^{-2.5} f''(c), \tag{11}$$

The Nusselt number is given by the following equation:

$$\mathrm{Re}_x^{-1/2} Nu_x = \left(-2c^{1/2} K_{nf} \big/ K_f\right)\theta'(c), \tag{12}$$

where$\mathrm{Re}_x = U_0 x/\nu_f$.

3. Results and discussion

The nonlinear Ordinary differential equations (ODE) [Eqs. (7) and (8)] with suitable restrictions [Eq. (9)] are unraveled by applying the Runge–Kutta-based shooting process. For computational purposes, the nondimensional constants are used throughout the study as $A^* = B^* = c = 0.1$; $\phi = 0.01; R = 0.5$; $M = 1; Ec = 0.1; \lambda = 1$. Figs. 2 and 3 represent the effect of the magnetic parameter (M) on the velocity and temperature descriptions. It has been noticed that as the value of the magnetic parameter (M) rises, the velocity description reduces and the temperature descriptions increase for both Sakiadis and Blasius motion cases. In general, larger values of M enhance the divergent force of motion known as the Lorentz force. This type of impact has a tendency to reduce the velocity profiles and increase the thermal boundary layers.

Figs. 4 and 5 display the effect of (ϕ) on the velocity and temperature descriptions, respectively, for both Sakiadis and Blasius motion investigations. It has been observed that the velocity decreases and temperature is enhanced as the increase in the volume fraction (ϕ) occurs for both Sakiadis and Blasius flow cases. Temperature descriptions for various values of nonuniform heat source/sink are illustrated in Figs. 6 and 7 for both Sakiadis and Blasius flow cases. It can be seen from the figures that an increase in the nonuniform heat source/sink parameters increases the temperature descriptions for both Sakiadis and Blasius flow cases. This is consistent with the common physical conduction in a heat source/sink where the non-negative values of (A^*) and (B^*) behave like heat generators, and negative values act as heat absorbers. Typically, enhancement of the heat source will exceed the thermal and velocity boundary layer thickness.

The temperature descriptions for various values of Eckert number are illustrated in Fig. 8 for Sakiadis and Blasius flow cases. It is noted that the temperature and thermal boundary layer thicknesses are enhanced by an increase in the values of Eckert number for both Sakiadis and Blasius flow investigations. This may be due to the increasing viscosity of the fluid. Figs. 9 and 10 show the effect of needle thickness parameter c on the velocity and temperature profiles, respectively, for both Sakiadis and Blasius flow investigations. It can be seen that the velocity and temperature descriptions decline with the increment in the needle parameter c for both Sakiadis and Blasius flow cases.

Tables 1 and 2 depict the variations in wall friction and local Nusselt number for the Sakiadis and Blasius flows. It is clear that the rising values of the volume fraction of the nanoparticles enhance the heat transfer rate of the Sakiadis flow. However, this trend is reversed for the Blasius flow. The increase in film thickness enhances the local Nusselt number in both cases. Increasing the magnetic field parameter reduces the wall friction. The uneven heat source/sink parameters reduce the heat transfer rate. Table 3 presents the thermal and physical properties. Table 4 shows the validation of the numerical procedure.

4. Conclusions

An analysis of the boundary layer of a two-dimensional forced convective flow along a persistent moving horizontal needle in an

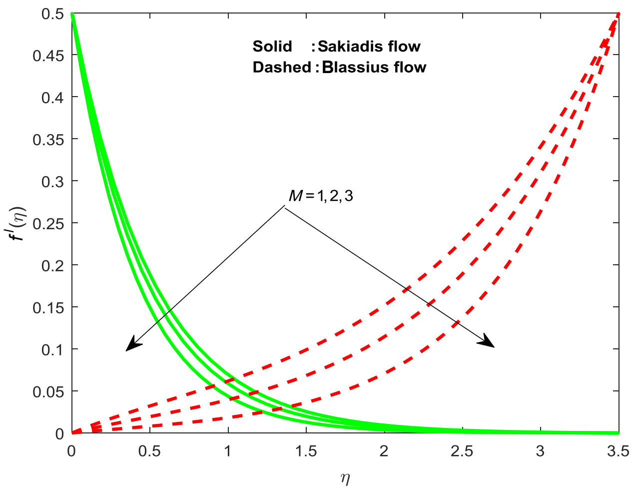

Fig. 2. Velocity profiles versus parameter *M*.

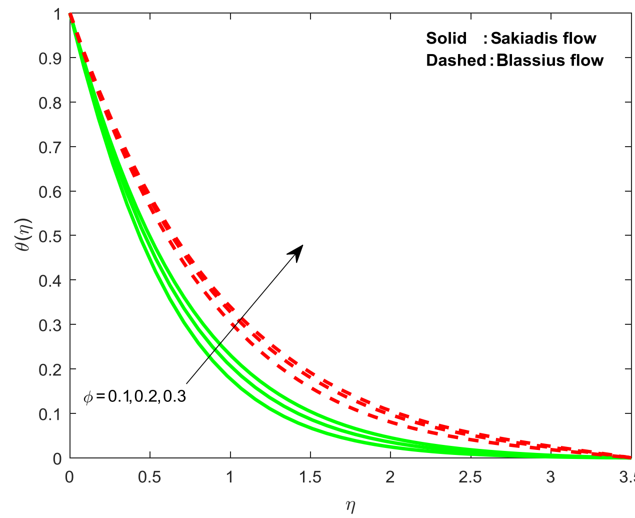

Fig. 5. Temperature profiles versus volumetric fraction ϕ.

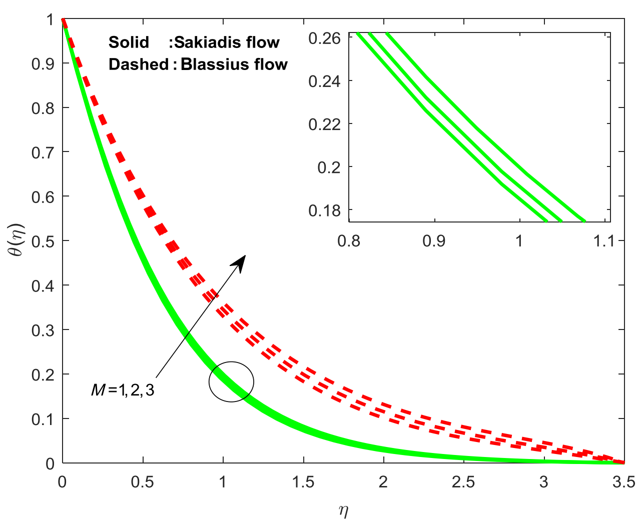

Fig. 3. Temperature profiles versus parameter *M*.

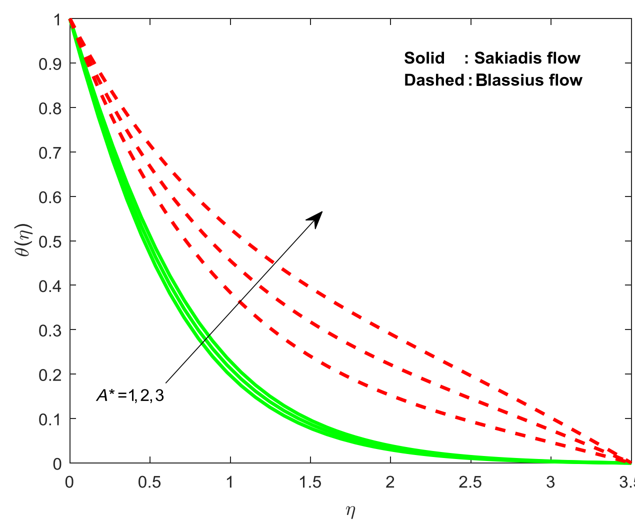

Fig. 6. Temperature profiles versus heat source/sink.

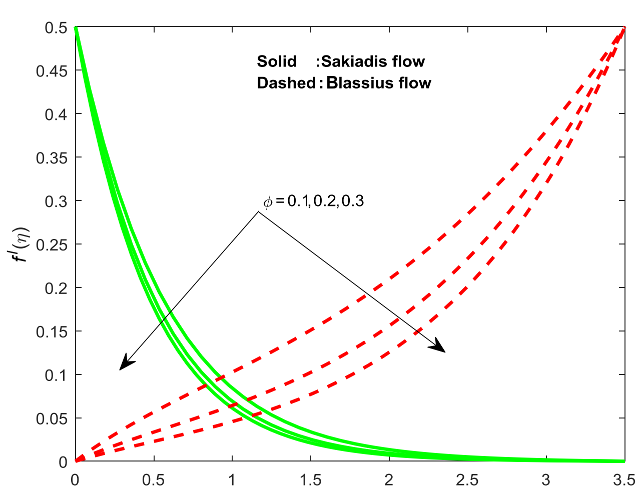

Fig. 4. Velocity profiles versus volumetric fraction ϕ.

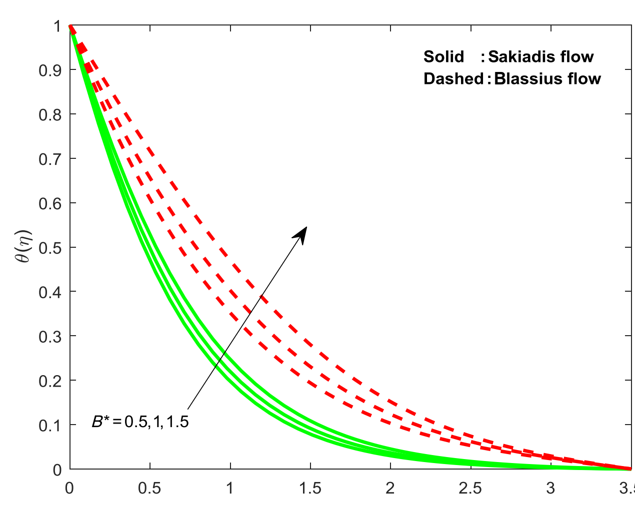

Fig. 7. Temperature description versus heat source/sink.

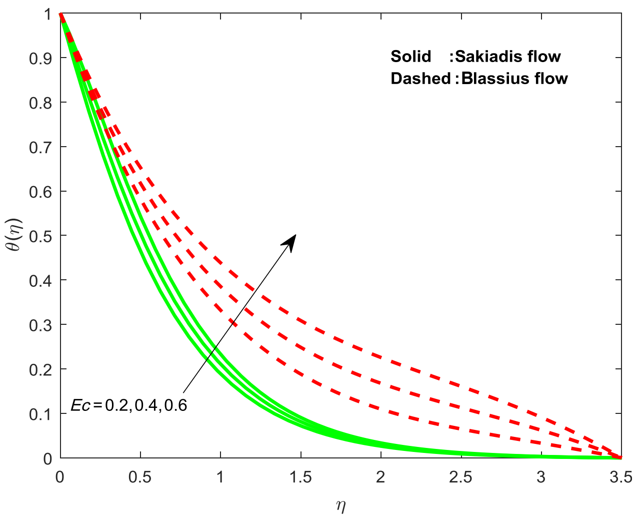

Fig. 8. Temperature description versus Eckert number.

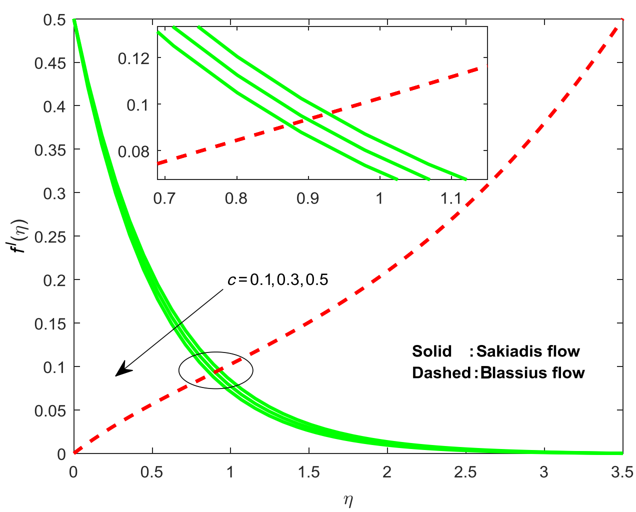

Fig. 9. Velocity profiles versus needle thickness.

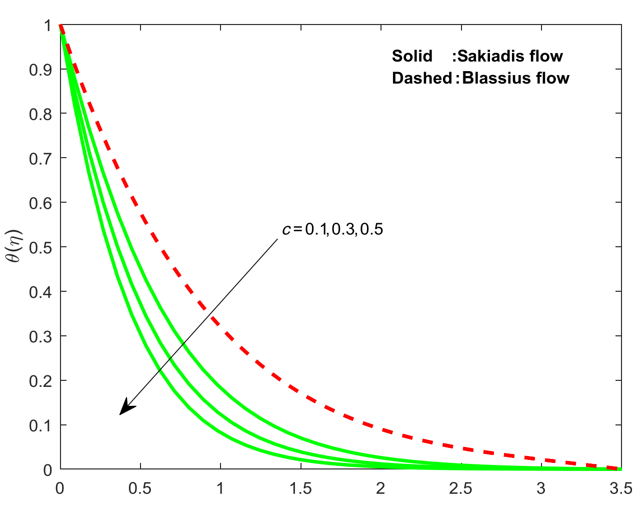

Fig. 10. Temperature profiles versus needle thickness.

Table 1
Variations in skin friction coefficient and rate of heat transfer for Sakiadis flow at various dimensionless parameters.

M	ϕ	Ec	A^*	B^*	c	$f''(0)$	$-\theta'(0)$
1.0						−1.588128	1.179495
2.0						−1.730070	1.150098
3.0						−1.975926	1.100856
	0.1					−1.426861	1.213765
	0.2					−2.132467	1.489423
	0.3					−3.170742	1.848360
		0.2				−1.426861	1.098226
		0.4				−1.426861	0.867145
		0.6				−1.426861	0.636065
			1			−1.426861	1.118156
			2			−1.426861	1.039048
			3			−1.426861	0.959939
				0.5		−1.426861	1.119728
				1.0		−1.426861	1.023608
				1.5		−1.426861	0.913876
					0.1	−1.426861	1.189354
					0.3	−2.994348	3.034660
					0.5	−4.151636	4.905788

Table 2
Variations in skin friction coefficient and rate of heat transfer for Blasius flow at various dimensionless parameters.

M	ϕ	Ec	A^*	B^*	c	$f''(0)$	$-\theta'(0)$
1.0						0.126476	0.898468
2.0						0.074871	0.876819
3.0						0.029832	0.853217
	0.1					0.227165	0.932990
	0.2					0.177012	1.179995
	0.3					0.165789	1.512313
		0.2				0.227165	0.893418
		0.4				0.227165	0.814273
		0.6				0.227165	0.735129
			1			0.227165	0.806046
			2			0.227165	0.701279
			3			0.227165	0.596512
				0.5		0.227165	0.803410
				1.0		0.227165	0.662989
				1.5		0.227165	0.491699
					0.1	0.227165	0.900338
					0.3	0.454330	1.800676
					0.5	0.601022	2.382071

Table 3
Thermal and physical properties.

Properties	Methanol	Cu
$\rho(\mathrm{kg/m^3})$	792	5,180
C_p(J/kg.K)	2,545	670
k (W/m.K)	0.2035	9.7
σ(S/m)	0.5×10^{-6}	0.74×10^{6}
Pr	7.38	—

Table 4
Validation of the numerical technique.

M	RKS	RKF	$bvp4c$	$bvp5c$
1	0.898468	0.898468314	0.898468313	0.898468313
2	0.876819	0.876819345	0.876819344	0.876819344
3	0.853217	0.853217871	0.853217870	0.853217870

electrically conducting MHD dissipative nanofluid was conducted. The energy equation was constructed with the Joule heating, viscous dissipation, and nonuniform heat source/sink effects. We analyzed the boundary layer behavior of a continuously moving needle in Blasius (moving fluid) and Sakiadis (quiescent fluid) flows. The findings are as follows:

- The boundary layer behaviors of the Sakiadis and Blasius flows are nonuniform.
- The heat transfer rate is high in the Sakiadis flow compared with that in the Blasius flow.
- The influence of the Lorentz force on the Sakiadis flow is high compared with that on the Blasius flow.
- Increasing the needle thickness enhances the heat transfer rate of both flows.
- The drag force caused by an external magnetic field reduces the wall friction.

Conflicts of interest

None declared.

References

[1] S.U.S. Choi, Enhancing thermal conductivity of fluids with nanoparticles, Proc. ASME Int. Mech. Eng. Cong. Exp. 66 (1995) 99–105.

[2] M. Agarwal, R.P. Chhabra, V. Eswaran, Laminar momentum and thermal boundary layers of power-law fluids over a slender cylinder, Chem. Eng. Sci. 57 (2002) 1331–1341.

[3] M. Kumari, G. Nath, Mixed convection boundary layer flow over a thin vertical cylinder with localized injection/surjection and cooling/heating, Int. J. Heat Mass Transfer 47 (2004) 969–976.

[4] A. Ishak, R. Nazar, I. Pop, Boundary layer flow over a continuously moving thin needle in a parallel free stream, Chin. Phys. Lett. 24 (2007) 2895–2897.

[5] S. Ahmad, N.M. Arifin, R. Nazar, I. Pop, Mathematical modeling of boundary layer flow over a moving thin needle with variable heat flux, in: 12th WSEAS International Conference on Applied Mathematics, ACM digital library, 2007, pp. 48–53.

[6] H.S. Takhar, A.J. Chamkha, G. Nath, Combined heat and mass transfer along a vertical moving cylinder with a free stream, Heat Mass Transfer 36 (2000) 237–246.

[7] T. Cebeci, T.Y. Na, Laminar free-convection heat transfer from a needle, Phys. Fluids 12 (1969) 463–465.

[8] P.M. Patil, S. Roy, I. Pop, Unsteady effects on mixed convection boundary layer flow from a permeable slender cylinder due to non-linearly power law stretching, Comput. Fluids 56 (2012) 17–23.

[9] R. Mehmood, S. Nadeem, S. Saleem, N.S. Akber, Flow and heat transfer analysis of a Jeffery nano fluid impinging obliquely over a stretched plate, J. Taiwan Inst. Chem. Eng. 74 (2017) 49–58.

[10] F.M. Hady, R. Mohamed, M.R. Abd-Elsalam, A. Mostafa Ahmed, The Blasius and Sakiadis flow in a nanofluids through porous medium in the presence of thermal radiation under a convective surface boundary condition, Int. J. Eng. Innov. Technol. 3 (2013) 225–243.

[11] O.D. Makinde, Analysis of Sakiadis flow of nanofluids with viscous dissipation and Newtonian heating, Appl. Math. Mech. 33 (2012) 1545–1554.

[12] O.D. Makinde, A. Aziz, Boundary layer flow of a nanofluid past a stretching sheet with a convective boundary condition, Int. J. Therm. Sci. 50 (2011) 1326–1332.

[13] N. Sandeep, V. Sugunamma, P. Mohan Krishna, Effects of radiation on an unsteady natural convection flow of a EG-Nimonic 80a nanofluids past an infinite vertical plate, Adv. Phys. Theor. Appl. 23 (2013) 36–43.

[14] P. Mohan Krishna, V. Sugunamma, N. Sandeep, Radiation and magnetic field effects on unsteady natural convection flow of a nanofluid past an infinite vertical plate with heat source, Chem. Process. Eng. Res. 25 (2014) 39–52.

[15] N. Sandeep, Effect of aligned magnetic field on liquid thin film flow of magnetic-nanofluid embedded with graphene nanoparticles, Adv. Powder Technol. 28 (2017) 865–875.

[16] P.O. Olanrewaju, J.A. Gbadeyan, O. Agboolanand, S.O. Abah, Radiation and viscous dissipation effects for the Blasius and Sakiadis flows with a convective surface boundary condition, Int. J. Adv. Sci. Technol. 2 (2010) 102–115.

[17] M. Awais, S. Saleem, T. Hayat, S. Irum, Hydromagnetic couple-stress nanofluid flow over a moving convective wall: OHAM analysis, Acta Astronaut 129 (2016) 271–276.

[18] V. Ambethkar, Numerical solutions of heat and mass transfer effects of an unsteady MHD free convective flow past an infinite vertical plate with constant suction, J. Naval Architect. Marine Eng. 5 (2008) 7–36.

[19] S. Nadeem, A.U. Khan, S. Saleem, A comparative analysis on different nanofluid models for the oscillatory stagnation point flow, Eur. Phys. J. Plus 131 (2016) 261.

[20] P. Mohan Krishna, V. Sugunamma, N. Sandeep, Effects of radiation and chemical reaction on MHD boundary layer flow over a moving vertical porous plate with heat source, Adv. Phys. Theor. Appl. 26 (2013) 109–128.

[21] S.Y. Ibrahim, O.D. Makinde, Chemically reacting MHD boundary layer flow of heat and mass transfer over a moving vertical plate with suction, Sci. Res. Essays 5 (2010) 2875–2882.

[22] M. Sulochana, M.K. Kishore Kumar, N. Sandeep, Influence of aligned magnetic field on the flow through vertical surface in porous medium with heat source, Adv. Phys. Theor. Appl. 42 (2015) 33–45.

[23] E. Jones, M. Pravin Brijgopal, K. Rohan Ravindra, N. Sandeep, Aligned magnetic field, radiation and chemical reaction effects on MHD boundary layer flow over a moving vertical porous plate, Chem. Process. Eng. Res. 31 (2015) 89–103.

[24] W.A. Khan, I. Pop, Boundary layer flow of a nanofluid past a stretching sheet, Int. J. Heat Mass Transfer 53 (2010) 2477–2483.

[25] K. Bhattacharya, S. Mukhopadhyay, G.C. Layek, Unsteady MHD boundary layer flow with diffusion and first order chemical reaction over a permeable stretching sheet with suction or blowing, Chem. Eng. Commun. 200 (2013) 379–397.

[26] G.K. Ramesh, B.J. Gireesha, C.S. Bagewadi, Convective heat transfer in a dusty fluid over a permeable surface with thermal radiation, Int. J. Nonlinear Sci. 14 (2012) 243–250.

[27] S. Sharidan, J. Mahmood, I. Pop, Similarity solutions for the unsteady boundary layer flow and heat transfer due to a stretching sheet, Int. J. Appl. Mech. Eng. 11 (2006) 647–654.

[28] S. Siddiqa, Gul-e-Hina, N. Begum, S. Saleem, M.A. Hossain, R.S.R. Gorla, Numerical solution of nanofluid bioconvection due to gyrotactic microorganisms along a vertical wavy cone, Int. J. Heat Mass Transfer 101 (2016) 608–613.

[29] M. Gnaneswara Reddy, N. Sandeep, Computational modelling and analysis of heat and mass transfer in MHD flow past the upper part of a paraboloid of revolution, Eur. Phys. J. Plus 132 (2017) 222.

[30] M. Jayachandra Babu, N. Sandeep, UCM flow across a melting surface in the presence of double stratification and cross-diffusion effects, J. Mol. Liquids 232 (2017) 27–35.

[31] G. Kumaran, N. Sandeep, Thermophoresis and Brownian moment effects on parabolic flow of MHD Casson and Williamson fluids with cross diffusion, J. Mol. Liquids 233 (2017) 262–269.